DOI: 10.1002/ejic.200701306

Facile Gram-Scale Growth of Single-Crystalline Nanotetrapod-Assembled ZnO Through a Rapid Process

Jianye Li,*[a,b] Hongying Peng,[c][‡] Jie Liu,*[a] and Henry O. Everitt[c,d]

Keywords: Nanocrystalline materials / Semiconducting materials / Nanotetrapods / Zinc oxide

From a rapid combustion and catalyst-free method, pure single-crystalline nanotetrapod-assembled bulk nano-ZnO was grown on a gram-scale for the first time. The gram-scale bulk nano-ZnO is synthesized from ZnO powder with great reliability and repeatability, and also a high conversion efficiency. All four arms of the nanotetrapods are cone shaped and grow in the [001] direction. The photoluminescence properties of the nanotetrapod-assembled ZnO were studied and a mechanism was suggested for the growth of the bulk nanotetrapod-assembled ZnO.

Introduction

Because of their wide bandgap, II–VI group compounds are very important semiconductors and widely used in optical and electro-optical devices. Among them, wurtzite-structured zinc oxide (ZnO) is an especially important II–VI group semiconductor with a direct wide bandgap of 3.37 eV at room temperature.[1–3] It has a large exciton binding energy (60 meV for ZnO vs. 28 meV for GaN) and a high optical gain (300 cm^{-1} for ZnO vs. 100 cm^{-1} GaN) at room temperature.[2,3] Wurtzitic ZnO is a very interesting material because of its applications in numerous fields. Its low voltage and short wavelength (green or green/blue) are applicable in electro-optical devices such as light-emitting diodes and laser diodes, and it can also be used as transparent ultraviolet (UV)-protection films, transparent conducting oxide materials, piezoelectric materials, electron-transport media for solar cells, chemical sensors, photocatalysts, and so forth.[1–5]

In recent years, a lot of attention has been focused on the study of ZnO-nanostructured materials for understanding fundamental optical properties, developing novel nanotechnological applications, and exploiting its significant potential for nano-optoelectronics. Nano-ZnO has been suggested to be the next most important nanomaterial after carbon nanotubes.[6] Up to now, a number of ZnO nanostructures such as nanowires, nanorods, nanotetrapods, nanoribbons, nanorings, nanosprings, nanonails, and nanohelices have been reported.[7,8] Usually, the reported nano-ZnO is catalytically grown and deposited on a substrate as a thin film. This method has some disadvantages that limit the extensive applications of the nano-ZnO: (1) For applications, the as-grown nano-ZnO needs to be removed and collected from the substrate by means of ultrasonic agitation etc., and the nano-ZnO could be damaged during the collection process; (2) The as-grown nano-ZnO could be contaminated during the growth process (by catalyst) or the collection process.

ZnO tetrapods are a common morphology for ZnO and they have been extensively studied.[9–15] Recently, individual ZnO nanotetrapods were designed as multiterminal sensors to detect light with different wavelengths, and the results indicate that these multiterminal sensors are remarkable optoelectronic devices that are sensitive to ultraviolet light, and are an advantage for distinguishing noise and increasing sensitivity.[16]

In this report, we demonstrate that from a facile combustion and catalyst-free method, pure single-crystalline nanotetrapods can be produced on the gram-scale for the first time. By this technique, gram-scale bulk nano-ZnO is reliably and repeatedly assembled from ZnO powder with a conversion rate of up to 58%. The gram-scale nanotetrapod-assembled ZnO is valuable for applications (the nanotetrapods are self-assembled into bulk nano-ZnO and very easy to collect), damage-free, and contamination-free. To the best of our knowledge, this is the first time that the gram-scale growth of nano-assembled, pure and single-crys-

[a] Department of Chemistry, Duke University,
Durham, North Carolina 27708, USA
E-mail: jyli@duke.edu
jliu@chem.duke.edu
[b] Department of Physical Chemistry, University of Science & Technology Beijing,
Beijing, China
[c] Department of Physics, Duke University,
Durham, North Carolina 27708, USA
[d] U.S. Army Aviation & Missile Research, Development & Engineering Center,
Redstone Arsenal, Alabama 35898, USA
[‡] Present address: GE Global Research Center,
Niskayuna, New York 12309, USA

talline tetrapod ZnO has been realized. This facile technique will greatly facilitate the large-scale industrial production of nano-ZnO.

Results and Discussion

Figure 1 is a photograph of the gram-scale nanotetrapod-assembled bulk ZnO, which shows that the white products have dimensions of several centimeters. Figure 1b is a representative low-magnification field emission scanning electron microscopy (FESEM) image of a fragment of the as-grown nanotetrapod-assembled ZnO. Figure 1c is a high-magnification FESEM image of the nanotetrapod-assembled ZnO and it indicates that the nanotetrapods have arm lengths of up to several microns. Furthermore, it clearly reveals that the nanotetrapods remain intact as the samples grow in size.

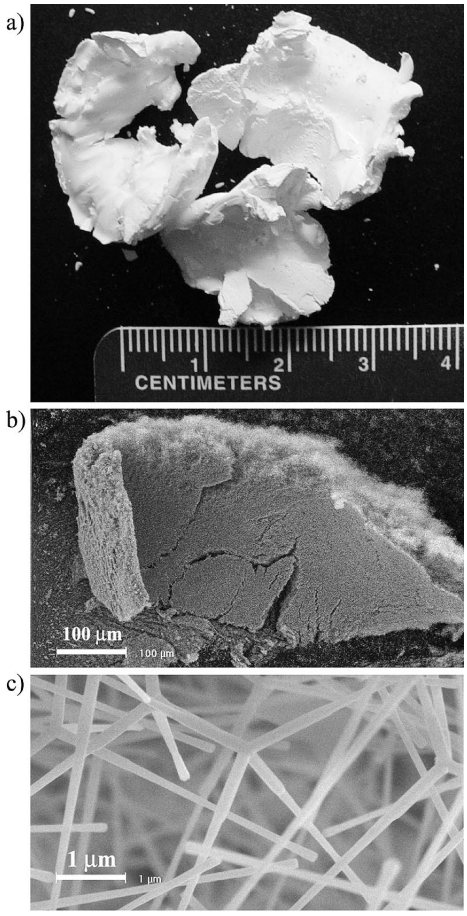

Figure 1. (a) Photograph of the gram-scale white nanotetrapod-assembled ZnO; (b) Representative low-magnification FESEM image from a fragment of the nanotetrapod-assembled ZnO (scale bar: 100 μm); (c) High-magnification FESEM image of the nanotetrapod-assembled ZnO (scale bar: 1 μm).

X-ray powder diffraction (XRD) was used to investigate the overall crystallographic properties and phase purity of the nanotetrapod-assembled ZnO. Figure 2 is a typical XRD pattern of the sample, and it can be indexed to a pure wurtzite structure of ZnO. These data are a good match to the standard values of hexagonal ZnO with lattice constants of a = 0.3250 nm and c = 0.5207 nm [joint committee on powder diffraction standards (JCPDS) card no. 36–1451]. The XRD result reveals that the products have a pure hexagonal wurtzite ZnO phase.

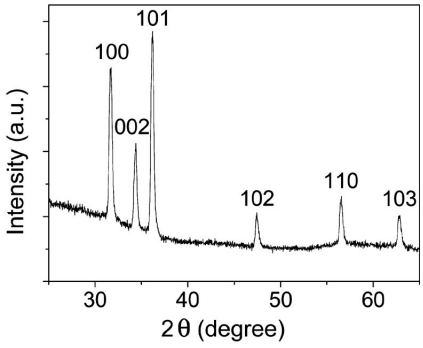

Figure 2. Room temperature XRD pattern of the nanotetrapod-assembled ZnO measured using Cu-K_α radiation.

Figure 3 shows a transmission electron microscopy (TEM) image of the ZnO nanotetrapods. All four arms of the nanotetrapods are cone shaped. The diameter of the arms at the center of the tetrapod is ca. 100 nm and at the tips it is ca. 20 nm.

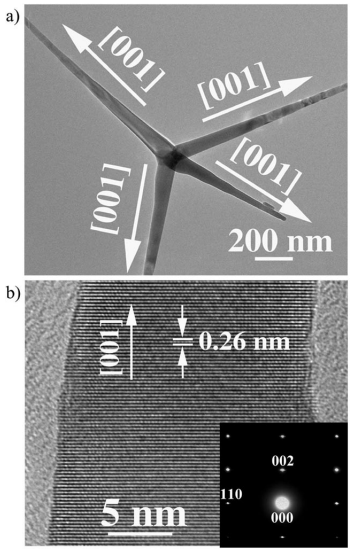

Figure 3. (a) TEM image of the ZnO nanotetrapod; (b) HRTEM image taken from an arm of the ZnO nanotetrapod (inset: SAED pattern of the arm of the nanotetrapod).

High-resolution TEM (HRTEM) and selected area electron diffraction (SAED) were used to further characterize the structure of the ZnO nanotetrapods. Part b of Figure 3 shows an HRTEM image taken from an arm of the nanotetrapod, and it clearly indicates the (001) atomic planes with an inter-planar spacing of 0.52 nm along the length of the arm. Furthermore, the HRTEM result reveals that the arms of the nanotetrapods are ideal single crystals without an amorphous shell. The SAED pattern on the arm of the ZnO nanotetrapod (inset of Figure 3, b) can be indexed as a standard single-crystalline hexagonal structure of ZnO,

which is in good agreement with the XRD and HRTEM results. The perfect lattice fringes and SAED pattern reveal the ideal monocrystalline hexagonal phase quality of the ZnO nanotetrapods. The HRTEM and SAED results also indicate that all four arms of the nanotetrapods grow along the [001] direction.

Curve (a) (gray) and curve (b) (black) in Figure 4 are the room temperature photoluminescence (PL) spectra measured from the nanotetrapod-assembled ZnO and commercial ZnO powders (99.99%, Alfa Aesar), respectively.

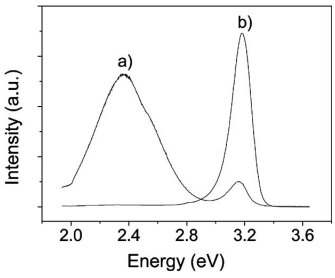

Figure 4. Room temperature photoluminescence spectra with excitation energy of 3.815 eV. (a) Nanotetrapod-assembled ZnO. (b) Commercial ZnO powders.

The emission at approximately 3.18 eV, near the ultraviolet (UV) band edge emission of ZnO (ca. 3.3 eV at 295 K),[19] occurs in both curves. This emission is generally attributed to the recombination of free excitons through an exciton–exciton collision process.[1] There is a broad below-bandgap emission centered at 2.37 eV in curve (a). The chemical and structural origins of this "green band" from ZnO are still a matter of debate. The most frequently cited explanation for the visible luminescence is that it arises from the recombination of photogenerated holes in the valence band with electrons trapped at deep-level, singly-ionized oxygen vacancies in ZnO.[17,18] Another frequently cited explanation is from the recombination of electrons in the conduction band and/or shallow donor states with holes trapped at oxygen vacancies.[17,19]

The green emission from tetrapod-structured ZnO has been observed by a lot of researchers[20–27] and the origin of the green luminescence is still a controversial issue. A couple of possible causes, such as intrinsic defects in ZnO (oxygen vacancy or Zn interstitials etc.)[20–24] and defects located at the surface[25,28] etc., of the green emission of ZnO tetrapods were proposed in the literature.

It can be seen from curve (a) that the "visible band" emission is much stronger than the UV band edge emission. Some researchers think that the high peak intensity ratio of the "visible band" emission to the UV band edge emission from nanostructured ZnO is due to the high surface-to-volume ratio of the ZnO nanostructures.[17,26,29] The phenomenon of the dependence of the visible emission on the diameter of ZnO nanowires has already been described in the literature.[29–31] Recently, He et al. found that the ZnO tetrapods with a high surface-to-volume ratio produced a stronger and wider green emission.[26] Zollfrank et al. demonstrated that the intensity of the green emission was dependent on the leg diameter of the ZnO tetrapods and the green emission increased with decreasing the leg diameter.[27]

There are three different growth mechanisms to explain the initial formation of the wurtzite-structured ZnO tetrapods.[32] The first one is based on the assumption of the existence of a zinc-blende phase core at the center of the wurtzite ZnO tetrapods;[33] the second one is built upon the octahedral multiple twin structure, giving a growth model from a multiple inversion-twin embryo and suggesting that the octahedral multiple inversion-twin formed first;[34] the third one is that the ZnO tetrapods grow from wurtzite-phased multiple twins induced in a zinc-blende structured nucleus, and that the zinc-blende phase nucleus only exists in the high-temperature tetrapods and will degenerate to multiple twins at room temperature.[35] Recently, Ding et al. directly observed the zinc-blende structure core in the initial formation of wurtzite ZnO nanotetrapods and confirmed the zinc-blende core in the nucleation of the wurtzite-structured ZnO tetrapods.[32]

After the nucleation of the wurtzite-structured ZnO nanotetrapods takes place, it appears that the arms of the nanotetrapods reported here prolong via a vapor–solid (VS) mechanism.[36–38] This is because no catalyst is used in the growing process, nor are catalyst particles detected at the arm tips. In vapor–liquid–solid (VLS) growth liquid catalyst particles act as the energetically favored sites for absorption of gas-phase reactants and catalyst particles are typically detected at tips of the one-dimensional materials.[39]

At the center of the tube furnace, ZnO powders inside a horizontal, fused quartz tube were reduced at high temperature by graphite carbon through a "carbon reduction" process, generating zinc vapor and CO.[30] The Zn vapor and CO were transported downstream by a flow of argon. Because of impurities in the argon and the leak of the growth system, a small amount of oxygen occurred in the tube. During the transportation process, the Zn vapor reacted with the oxygen to form ZnO. Accompanied by the zinc, the ZnO deposited to form a grayish zinc-mixed ZnO material at the relatively low-temperature zone of the tube. Because zinc has a lower boiling point than zinc oxide, the distance between the source (ZnO/graphite carbon powders) and the depositing sites has a strong effect on the zinc level in the mixture. The further the depositing site (lower-temperature zone) from the source, the more zinc was found in the mixture, as revealed by the energy dispersive X-ray (EDX) (see Figure 5, parts a and b).

When the downstream end of the tube was opened and the as-grown grayish material was heated under the flow of argon at 740–820 °C, the zinc component in the mixture was quickly burnt with bluish green flames and the mixture completely changed to pure ZnO vapor. By the flow of argon, this ZnO vapor was transported to the downstream end of the tube. At this low-temperature area, the ZnO vapor deposited and nucleation of the wurtzite-structured ZnO nanotetrapods took place. Through a vapor–solid (VS) growth process,[36–38] the arms of the nanotetrapods prolonged. Because of the rapid deposition at the down-

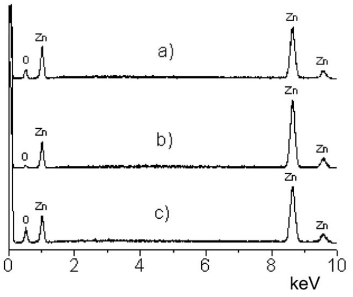

Figure 5. EDX of (a) zinc-mixed ZnO deposited at a site with a shorter distance from the source; (b) zinc-mixed ZnO deposited at a site with a longer distance from the source; and (c) pure gram-scale nanotetrapod-assembled ZnO.

stream end of the tube, the nanotetrapods assembled quickly to form the gram-scale nanotetrapod-assembled bulk nano-ZnO. The EDX measurement of the nanotetrapod-assembled ZnO (Figure 5, c) shows a 1:1 Zn:O composition, consistent with stoichiometric ZnO, revealing that the nanotetrapods are composed of pure ZnO. Rapid burning of the grayish material under the flow of argon is thus the key step to producing the large-scale nanotetrapod-assembled bulk nano-ZnO.

Conclusions

In summary, we have developed a simple, facile, and catalyst-free method for gram-scale growth of pure single crystalline nanotetrapod-assembled bulk nano-ZnO. The structure of the ZnO nanotetrapods was characterized. All four arms of the as-grown ZnO nanotetrapods are cone shaped and grow in the [001] direction. The photoluminescence of the ZnO nanotetrapods shows a high intensity "visible band" emission. The high peak intensity ratio of the "visible band" emission to the UV band edge emission is due to the high surface-to-volume ratio of the ZnO nanotetrapods. A mechanism is suggested for the growth of the nanotetrapod-assembled ZnO. When using this highly repeatable technique the gram-scale growth of nano-assembled bulk nano-ZnO from ZnO powder occurs with a high conversion rate. This is the first time that the gram-scale growth of single-crystalline ZnO nanotetrapods and nanostructure-assembled bulk nano-ZnO has been realized. This facile approach could also be applicable for preparing other nanomaterial-assembled oxides, opening up more opportunities for fundamental studies and greatly facilitating the large-scale industrial applications of nanomaterials.

Experimental Section

The nanotetrapod-assembled ZnO was grown in a horizontal, fused quartz tube inside a tube furnace previously used to prepare GaN nanowires.[40] The source material was a mixture of ZnO (99.99%, Alfa Aesar) and graphite carbon powders (99.9995%, Alfa Aesar) with a weight ratio between 1:1 and 2:1. First, the raw material was loaded into a fused quartz boat, and the boat was placed into the horizontal fused quartz tube with the source material located at the center (the highest temperature zone) of the tube furnace. Then the furnace was heated under a steady flow of argon (99.99%, National Specialty Gases) of 100–200 standard cubic centimeters per minute (sccm). When 980–1080 °C was reached, the temperature was kept constant for 6–10 h. Grayish material completely covered the inner wall of the downstream section of the tube. The temperature was then quickly decreased to 740–820 °C, after which the downstream end of the tube was opened and the downstream part with grayish material was moved to the center of the tube furnace. The grayish material remained there for 1–3 min before being burnt completely. After that, the furnace was switched off and opened, and then quickly cooled to room temperature. Gram-scale white nanotetrapod-assembled ZnO was obtained in the area near the downstream end of the tube, and up to 58% of the ZnO powder in the original source was converted into nano-assembled products.

The as-grown gram-scale nano-ZnO was characterized by field emission scanning electron microscopy (FESEM, Philips FEI XL30SFEG), X-ray powder diffraction (XRD, Rigaku Multiflex X-ray diffractometer with Cu-K_α radiation at room temperature), transmission electron microscopy (TEM, Hitachi HF-2000), and photoluminescence [PL, He–Cd laser operating at 3.815 eV (325 nm)].

Acknowledgments

This work was partly supported by the Air Force Office of Scientific Research (AFOSR), Grant no. 49620-02-1-0188.

[1] M. H. Huang, S. Mao, H. Feick, H. Q. Yan, Y. Wu, H. Kind, E. Weber, R. Russo, P. D. Yang, *Science* **2001**, *292*, 1897–1899.
[2] E. M. Wong, P. C. Searson, *Appl. Phys. Lett.* **1999**, *74*, 2939–2941.
[3] S. Choopun, R. D. Vispute, W. Noch, A. Balsamo, R. P. Sharma, T. Venkatesan, A. Iliadis, D. C. Look, *Appl. Phys. Lett.* **1999**, *75*, 3947–3949.
[4] E. A. Meulenkamp, *J. Phys. Chem. B* **1998**, *102*, 5566–5572.
[5] J. Y. Lao, J. G. Wen, Z. F. Zen, *Nano Lett.* **2002**, *2*, 1287–1291.
[6] Z. L. Wang, X. Y. Kong, Y. Ding, P. X. Gao, W. L. Huges, R. S. Yang, Y. Zhang, *Adv. Funct. Mater.* **2004**, *14*, 944–956.
[7] C. Klingshirn, *ChemPhysChem* **2007**, *8*, 782–803.
[8] L. Schmidt-Mende, J. L. MacManus-Driscoll, *Mater. Today* **2007**, *10*, 40–48.
[9] M. Kitano, T. Hamabe, S. Maeda, *J. Cryst. Growth* **1990**, *102*, 965–973.
[10] H. Q. Yan, R. H. He, J. Pham, P. D. Yang, *Adv. Mater.* **2003**, *15*, 402–405.
[11] Z. Chen, Z. W. Shan, M. S. Cao, L. Lu, S. X. Mao, *Nanotechnology* **2004**, *15*, 365–569.
[12] A. B. Djurišić, W. C. H. Choy, V. A. L. Roy, Y. H. Leung, C. Y. Kwong, K. W. Cheah, T. K. Gundu Rao, W. K. Chan, H. Fei Lui, C. Surya, *Adv. Funct. Mater.* **2004**, *14*, 856–864.
[13] J. Zhang, Y. Yang, B. Xu, F. Jiang, J. Li, *J. Cryst. Growth* **2005**, *280*, 509–515.
[14] Z. X. Zhang, H. J. Yuan, Y. Gao, J. X. Wang, D. F. Liu, J. Shen, L. F. Liu, W. Y. Zhou, S. S. Xie, X. Wang, X. Zhu, Y. C. Zhao, L. F. Sun, *Appl. Phys. Lett.* **2007**, *90*, 153116.
[15] A. M. Fischer, S. Srinivasan, R. Garcia, F. A. Ponce, S. E. Guaño, B. C. Di Lello, F. J. Moura, I. G. Solórzano, *Appl. Phys. Lett.* **2007**, *90*, 121905.
[16] Z. X. Zhang, L. F. Sun, Y. C. Zhao, Z. Liu, D. F. Liu, L. Cao, B. S. Zou, W. Zhou, C. Gu, S. Xie, *Nano Lett.* **2008**, *8*, 652–655.
[17] J. V. Foreman, J. Y. Li, H. Y. Peng, S. J. Choi, H. O. Everitt, J. Liu, *Nano Lett.* **2006**, *6*, 1126–1130.

[18] K. Vanheusden, W. L. Warren, C. H. Seager, D. R. Tallant, J. A. Voigt, B. E. Gnade, *J. Appl. Phys.* **1996**, *79*, 7983–7990.
[19] A. van Dijken, E. A. Meulenkamp, D. Vanmaekelbergh, A. Meijerink, *J. Phys. Chem. B* **2000**, *104*, 1715–1723.
[20] W. D. Yu, X. M. Li, X. D. Gao, P. S. Qiu, W. X. Cheng, D. L. Ding, *Appl. Phys. A* **2004**, *79*, 453–456.
[21] V. A. L. Roy, A. B. Djurišić, H. Liu, X. X. Zhang, Y. H. Leung, M. H. Xie, J. Gao, H. F. Lui, C. Surya, *Appl. Phys. Lett.* **2004**, *84*, 756–758.
[22] W. D. Yu, X. M. Li, X. D. Gao, *Appl. Phys. Lett.* **2004**, *84*, 2658–2660.
[23] M. N. Jung, S. Y. Ha, S. H. Park, M. Yang, H. S. Kim, W. H. Lee, T. Yao, J. H. Chang, *Phys. E* **2006**, *31*, 187–190.
[24] M. Kaur, S. Bhattacharya, M. Roy, S. K. Deshpande, P. Sharma, S. K. Gupta, J. V. Yakhmi, *Appl. Phys. A* **2007**, *87*, 91–96.
[25] A. B. Djurišić, W. M. Kwok, Y. H. Leung, D. L. Phillips, W. K. Chan, *J. Phys. Chem. B* **2005**, *109*, 19228–19233.
[26] F. Q. He, Y. P. Zhao, *J. Phys. D: Appl. Phys.* **2006**, *39*, 2105–2108.
[27] C. Zollfrank, C. R. Rambo, M. Batentschuk, P. Greil, *J. Mater. Sci.* **2007**, *42*, 6325–6330.
[28] W. M. Kwok, A. B. Djurišić, Y. H. Leung, W. K. Chan, D. L. Phillips, *Appl. Phys. Lett.* **2005**, *87*, 223111.
[29] I. Shalish, H. Temkin, V. Narayanamurti, *Phys. Rev. B* **2004**, *69*, 245401.
[30] M. H. Huang, Y. Y. Wu, H. Feick, N. Tran, E. Weber, P. D. Yang, *Adv. Mater.* **2001**, *13*, 113–116.
[31] S. J. Chen, Y. C. Liu, Y. M. Lu, J. Y. Zhang, D. Z. Shen, X. W. Fan, *J. Cryst. Growth* **2006**, *289*, 55–58.
[32] Y. Ding, Z. L. Wang, T. Sun, J. Qiu, *Appl. Phys. Lett.* **2007**, *90*, 153510.
[33] M. Shiojiri, C. Kaito, *J. Cryst. Growth* **1981**, *52*, 173–177.
[34] M. Fujii, H. Iwanaga, M. Ichihara, S. Takeuch, *J. Cryst. Growth* **1993**, *134*, 275–280.
[35] K. Nishio, T. Isshiki, M. Kitano, M. Shiojiri, *Philos. Magn. A* **1997**, *76*, 889–904.
[36] P. D. Yang, C. M. Lieber, *J. Mater. Res.* **1997**, *12*, 2981–2996.
[37] C. Liu, Z. Hu, Q. Wu, X. Z. Wang, Y. Chen, H. Sang, J. M. Zhu, S. Z. Deng, N. S. Xu, *J. Am. Chem. Soc.* **2005**, *127*, 1318–1322.
[38] J. Y. Li, X. L. Chen, *Solid State Commun.* **2004**, *131*, 769–772.
[39] A. M. Morales, C. M. Lieber, *Science* **1998**, *279*, 208–211.
[40] J. Y. Li, C. G. Lu, B. Maynor, S. M. Huang, J. Liu, *Chem. Mater.* **2004**, *16*, 1633–1636.

Received: December 4, 2007
Published Online: June 3, 2008

